Turkish Journal of Chemistry

http://journals.tubitak.gov.tr/chem/

Research Article

Turk J Chem
(2014) 38: 617 – 628

doi:10.3906/kim-1309-55

# Organic biomolecules bind to phosphate through borate linkages in aqueous solutions

**Nazik AYDOĞMUŞ[1], Dursun Ali KÖSE[2,*], Michael Andrew BECKETT[3], Birgül ZÜMREOĞLU KARAN[1,*]**

[1]Department of Chemistry, Hacettepe University, Beytepe Campus, Ankara, Turkey
[2]Department of Chemistry, Hitit University, Ulukavak, Çorum, Turkey
[3]School of Chemistry, Bangor University, Bangor, UK

**Received:** 23.09.2013 • **Accepted:** 22.01.2014 • **Published Online:** 11.06.2014 • **Printed:** 10.07.2014

**Abstract:** Solutions of salicyclic, ascorbic, and citric acids were reacted with boric acid, followed by $NaH_2PO_4$. The products, triphosphateborate ester of salicylic acid (**1**), orthosphateborate ester of ascorbic acid (**2**), triphosphateborate ester of ascorbic acid (**3**), and orthosphateborate ester of citric acid (**4**), were flash precipitated with cold acetone and characterised by microanalysis, thermal analysis, FT-IR, Raman, $^{11}$B NMR, $^{31}$P MAS NMR, and mass spectroscopic techniques. Analytical results indicated the presence of –C–O–B–O–P– linkages with the attached phosphate groups varying between orthophosphate and triphosphate, depending on the starting material. The biomolecules studied in this work may serve as models in the B–P-organic system and the results would provide a possible contribution to boron prebiotic chemistry.

**Key words:** Borate complex, phosphate ester, boric acid, $^{31}$P MAS NMR, $^{11}$B NMR

## 1. Introduction

The question of how biological life emerged from inorganic matter through natural processes and the role of inorganic ions in the synthesis of simple organic molecules have been the subject of several hypotheses and laboratory studies.[1,2] Commonly accepted models for the prebiotic world emphasise the requirement of negatively charged ions such as carbonate, cyanide, ferrocyanide, phosphate, sulphide, and sulphite as sources of biomolecules.[3,4] Among these anionic species, phosphate ions are of particular importance in the prebiotic synthesis of products containing one or more phosphate groups able to oligomerise to sugar phosphates and further polymerise to RNA molecules.[5] Selective concentration of phosphate species, stabilisation of ribose, and catalytic synthesis of organic molecules under prebiotic conditions most likely proceeded over reactive surfaces of the rocks and minerals present in the oceans. It has been suggested that borate minerals could have played a crucial role by stabilising the cyclic ribose during RNA synthesis.[6–8] A potential and catalytic role of boric acid in peptide and nucleic acid synthesis[9] and stabilisation of sugar molecules by acting as a complexing agent[10,11] have been demonstrated. Recently, thermal condensation of formamide in the presence of borate minerals has been shown to form nucleic acid precursors.[12] Holm et al.[13] proposed that brucite mineral (solid $Mg(OH)_2$) may scavenge borate and phosphate from sea water. Brucite with adsorbed phosphate may catalyse the synthesis of pyrophosphate from orthophosphate, high pH conditions promote the abiotic formation of ribose, and ribose can be stabilised by borate leaving available positions for phosphorylation.

*Correspondence: dalikose@hitit.edu.tr, bkaran@hacettepe.edu.tr

Stimulated by the above-mentioned prebiotic scenarios, we explored the possibility of binding organic molecules to phosphate groups through borate ester linkages in aqueous solutions. Both boric acid and phosphoric acid are known to form ester structures with organic molecules through condensation reactions. Compounds containing B–O–P fragments prepared from boranes with phosphoric acid derivatives have been reported.[14] However, B–O–P bonding in aqueous media is limited to borophosphate formation in hydrothermal conditions,[15–18] to the best of the authors' knowledge. In this paper, we present evidence that such compounds are formed in solutions containing boric acid, $NaH_2PO_4$, and carboxylic acid derivatives. Salicylic acid was chosen as the probe molecule for reaction optimisation because of its well-defined esterification sites with boron[19,20] phosphorus.[21] The knowledge obtained with salicylic acid was then utilised in reactions with other carboxylic acids in order to obtain more information about the general applicability of the method. Our attention was drawn to ascorbic acid (a sugar acid with the same furanose ring as ribose) and citric acid (an important intermediate in the citric acid cycle), expecting further support for the formation of –C–O–B–O–P– linkages in aqueous solutions with carboxylic acid derivatives of biochemical importance.

## 2. Results and discussion

The experimental strategy was based on the formation of borate monoester of the biomolecule first, which undergoes further condensation with the added dihydrogenphosphate (Scheme 1). Because borate formation is reversible, $H_3BO_3$ was added in solid form to avoid confusion between interacting trigonal and tetrahedral boron species. No pH adjustment was made as the measured pH ($\leq 5$) of the mixture throughout the reaction course was optimal for complexation of boric acid with hydroxycarboxylic acids, according to the rules formulated by Van Duin et al.[22]

Chemical and thermogravimetric analysis data allowed the proposal of formulae for the compounds with salicylic (**1**), ascorbic (**2** and **3**), and citric acids (**4**) (Figure 1). Although the products were obtained by flash precipitation from aqueous solutions, the chemical compositions and hydrate water contents were shown to be in good agreement with the experimental values.

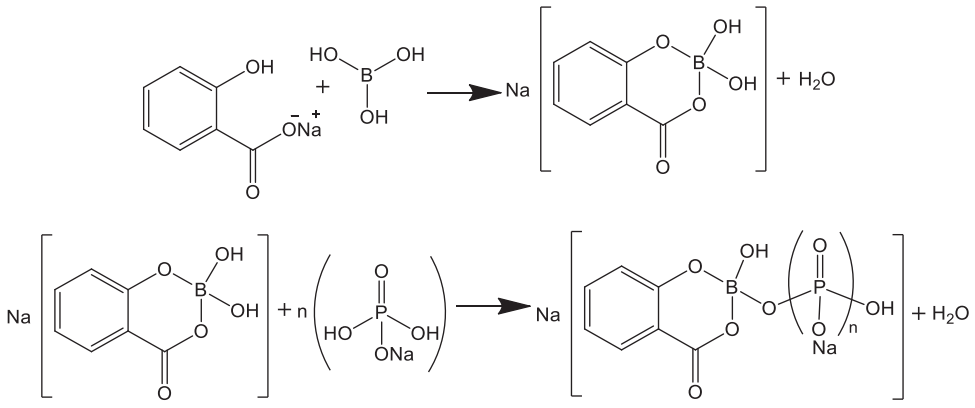


**Scheme 1.** Proposed formation of phosphateborate esters of salicylic acid.

The spectral data that will be discussed hereafter suggested the presence of linear B–O–$(PO_3Na)_n$ linkages in the products, with $n$ increasing with the employed phosphate ratio in the preparation step. The length of the phosphate chain increased with the amount of $NaH_2PO_4$ added to the reaction medium or conducting the reactions in high amounts of water. In such cases, no further detailed characterisation was

performed as the products containing a higher degree of phosphate polymerisation likely consist of mixtures with variable chain lengths.[23]

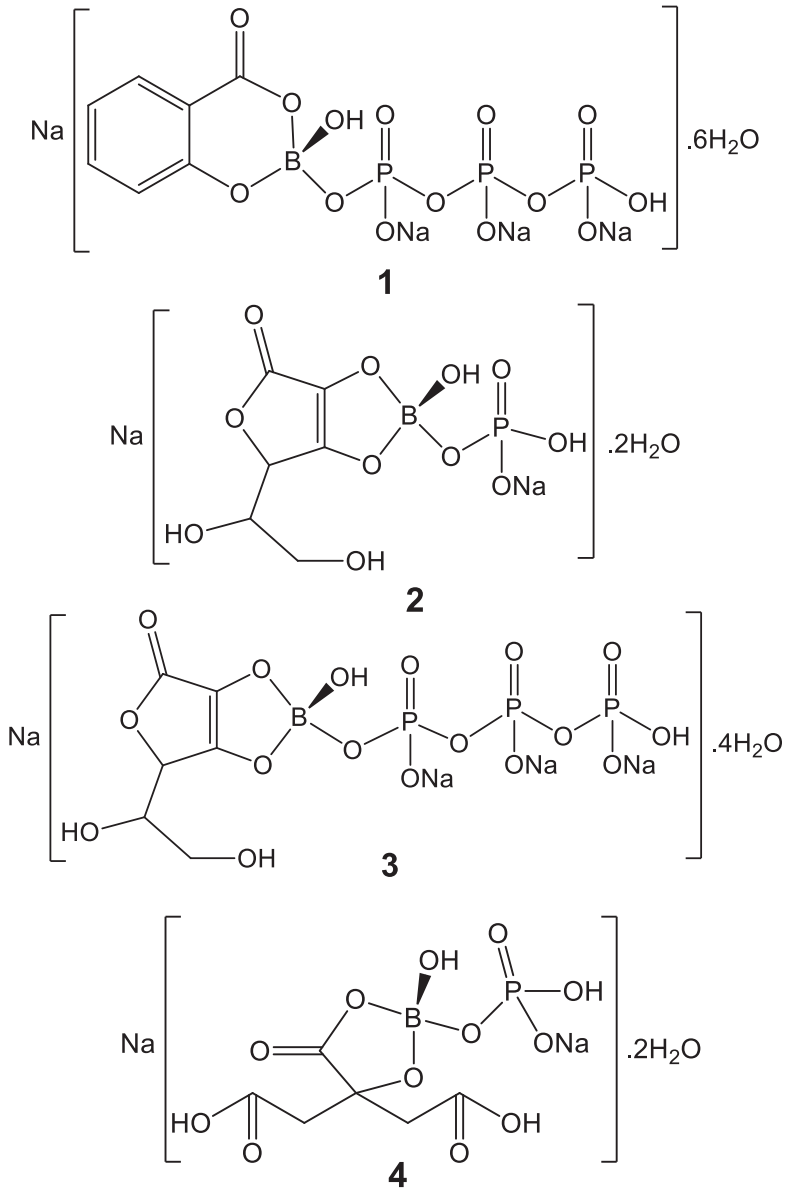


**Figure 1.** Schematic drawings of the triphosphateborate ester of salicyclic acid (**1**), the orthophosphateborate ester of ascorbic acid (**2**), the triphosphateborate ester of ascorbic acid (**3**), and the orthophosphateborate ester of citric acid (**4**).

The phosphorus atoms in the products were defined according to the common classification for non-equivalent phosphorus atoms in polyphosphates.[24–26] The Table summarises the symbols used in this article for terminal, internal, and boron-bridging phosphorus atoms, and introduces $Q^2_B$ for pseudo $Q^2$ species, in which a central P atom is bound to B and P via O atom linkages, and $Q^1_B$ for species, in which a terminal P atom is bound to B.

**Table.** Classification of phosphorus atoms in the products.

| | | |
|---|---|---|
| $\mathbf{Q^1}$ terminal | $PO(OP)O_2^{2-}$ | 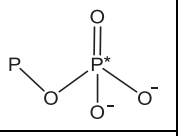 |
| $\mathbf{Q^2}$ internal | $PO(OP)_2O^-$ | 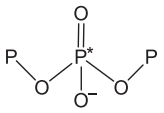 |
| $\mathbf{Q^1_B}$ Boron-bridging, terminal | $PO(OB)(O^-)_2$ | 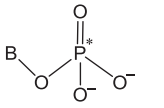 |
| $\mathbf{Q^2_B}$ Boron-bridging, internal | $PO(OP)(OB)O^-$ | 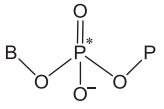 |

### 2.1. Phosphateborate esters of salicylic acid

Figure 1 displays the structure proposed for **1** (details of preparation are given in the experimental part) which contains a triphosphate chain attached to the borate group. FT-IR, Raman, $^{11}$B NMR, $^{31}$P MAS NMR and mass spectroscopic techniques confirmed the presence of –C–O–B–O–P– ester linkage in **1**. It was difficult to make a definitive assignment for B–O–P bonding from the FTIR spectrum because phosphate and borate peaks overlapped in the region 1250–850 cm$^{-1}$.[27] The Raman spectrum (Figure 2) showed more supporting evidence for B–O–P bonding in agreement with the proposed structure. The strongest band at 641 cm$^{-1}$ was attributed to $\nu_s$(POP) of the bridging oxygen atoms and the small peak at 995 cm$^{-1}$ was attributed to $Q^1\nu_a(PO_3)$.[28,29] B–O–P vibrations that give weak Raman signals might have been masked by the $\nu_s$(POP) peak. B–O stretching vibrations characteristic for 6-membered borate rings might have blue-shifted from 700 cm$^{-1}$ 30 due to the presence of the attached phosphate chain and overlapped with the strong peak at 641 cm$^{-1}$. A similar pattern has been observed in the Raman spectra of some borophosphate glasses.[26,31] The bands at 1167 cm$^{-1}$ and 590 cm$^{-1}$ were assigned to $Q^2\nu_s(PO_2)$ and to the bending modes of the orthophosphate groups, respectively. These P–O bands referring to nonbridging $PO_2$ groups were relatively weak as generally reported for borophosphate compounds.[32]

Figure 3 shows the $^{31}$P MAS-NMR spectrum of **1**. Solid-state $^{31}$P MAS-NMR spectroscopy is a useful tool for studying the structures of polyphosphates, borophosphates, and phosphate glasses. Inorganic polyphosphates generally give signals in the negative region of the spectra with high degrees of rotational side bands.[33,34] Normally, the $Q^2$ and $Q^1$ resonances of polyphosphate structures appear at $-20$ to $-30$ ppm and 0 to $-10$ ppm, respectively. Together with their corresponding side bands $(*)$, they broaden, shift, and overlap on $B_2O_3$ addition to phosphate glasses.[23,26,33–37] $^{11}$B$\{^{31}$P$\}$ and $^{31}$P$\{^{11}$B$\}$ rotational echo double resonance NMR (REDOR) experiments have shown that successive substitution of phosphate by borate produces a pronounced downfield shift trend in the spectra due to the increased formation of B–O–P linkages.[38] Shah et al.[36] have observed a ca. 20 ppm downfield shift for $Q^2$ by increasing the $B_2O_3$ content from 5 mol% to 20 mol% in phosphate glasses. Similar high-frequency shifts have been also observed in related $^{29}$Si spectra

with pseudo $Q^2_B$ environments.[39] In accord with these spectral features, the strong centre band observed in the spectrum of **1** at 20–25 ppm was identified as the $Q^2$ resonance with shoulders assigned to $Q^1$ and $Q^2_B$. A remarkable downfield shift was observed for changing a $Q^2$ to a $Q^2_B$ environment due to the presence of the boron atom and the aromatic ring in close proximity.

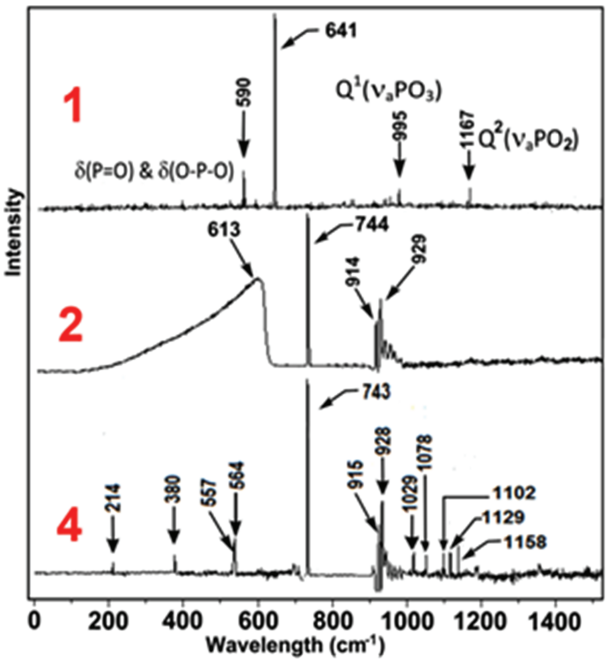


**Figure 2.** Raman spectra of **1**, **2**, and **4**.

The $^{11}$B NMR spectrum of **1** in $D_2O$ showed 2 major peaks at ca. +19.2 and +3.0 ppm (Figure 4). The solution $^{11}$B NMR spectra of boron–oxygen compounds generally give 2 peaks in the relatively narrow chemical shift range of $\delta$= 0–20 ppm[40] where the sharp peaks at high field are assigned as tetrahedral boron ($B_4$) and the others at low field as trigonal boron ($B_3$).[41,42] The appearance of 2 signals in the spectrum of **1** indicated that the product undergoes partial hydrolysis in $D_2O$ upon disruption of the B–O–P linkages, leading to an equilibrium between the parent tetrahedral borate and hydrolytic trigonal borate species.

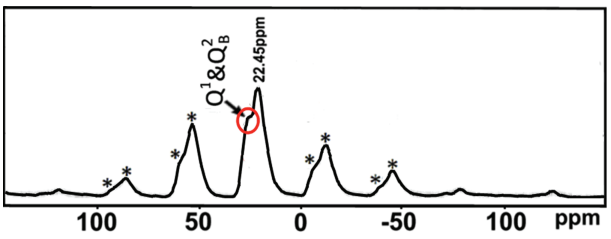


**Figure 3.** $^{31}$P MAS NMR spectrum of **1**.

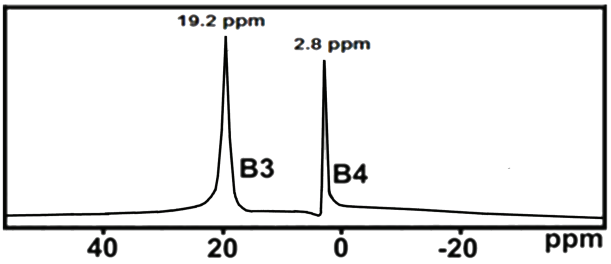


**Figure 4.** $^{11}$B MAS NMR spectrum of **1** in $D_2O$.

The observed fragmentation sequences in the mass spectrum of **1** correlated with the pathways suggested in Scheme 2. Considering trisodium-triphosphateborate ester of salicylic acid as the precursor ion (**1**-6$H_2O$-2$Na^+$ = 486 Da), the loss of terminal $Na^+$ and $H_2PO_4^-$ ions and elimination of the hydroxyl group on borate

were followed by sequential degradation of the remaining part (368 Da) to give the product ions at $m/z$ 303, 264, 236, and 164 Da.

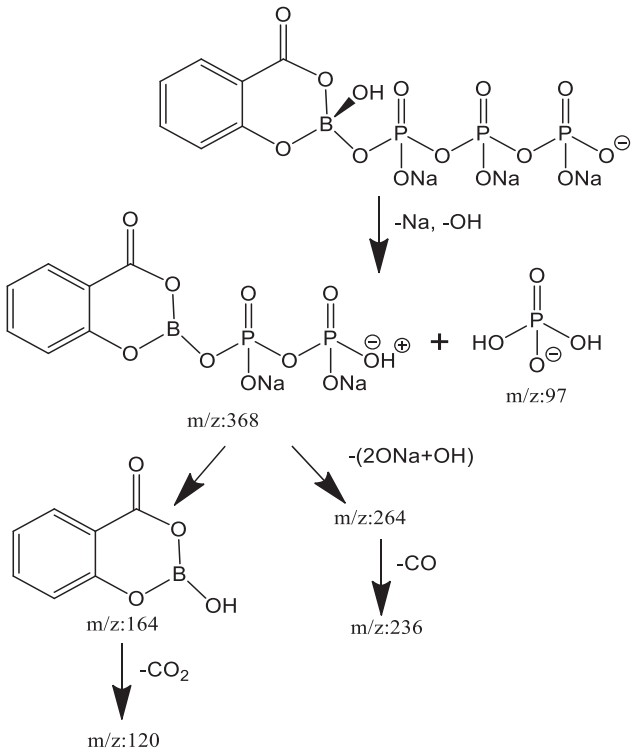


**Scheme 2.** Main fragmentation pathways for **1**.

Thermal stability of **1** was examined by recording the TGA curve in the range 25–800 °C. The observed thermogravimetric behaviour was the same as reported for borate esters of salicylic acid,[19,20] proceeding in the following order: removal of crystal water molecules at low temperatures, intramolecular water elimination at ca. 175 °C, and finally degradation of the organic group around 400 °C. **1** displayed a higher thermal stability with respect to pure salicylic acid for which the decomposition onset temperature was recorded as 110 °C. Salicylic acid forms a 6-membered ring with boric acid that not only enhances the thermal stability but also the hydrolytic stability of the ester structure.[43]

### 2.2. Phosphateborate esters of ascorbic acid

Ascorbic acid is a sugar acid with a *cis*-enediol group on the sugar ring and adjacent alcoholic hydroxy groups on the side chain available for complex formation with boric acid. Based on a similar chemistry to the salicyclic acid system, the proposed structures for the products (details of preparation of **2** and **3** are given in the experimental part) of the ascorbic acid–boric acid–sodium dihydrogenphosphate system are given in Figure 1. **2** was assigned as an orthophosphate and **3** as a triphosphate.

The FTIR spectra of **2** and **3**, together with that of sodium ascorbatoborate,[11] are shown in Figure 5. Broadening and small peak shifts were observed in the spectrum of sodium ascorbatoborate in the region 1300–800 $cm^{-1}$ due to overlapping $\nu_a$(B–O), $\nu_a$(P–O), $\nu_s$(P–O), ascorbate ring modes, and B–O–P vibrations, when a single phosphate group was linked to borate. P–O bands intensified, B–O bands weakened, and $\nu_a$(P–O–P)

appeared at 964 $cm^{-1}$ on moving from orthophosphate (**2**) to the triphosphate (**3**).[44,45] The Raman spectrum of **2** (Figure 2) was also in agreement with the structure proposed in Figure 1. The absence of the $Q^2$ band at 1167 $cm^{-1}$ indicated that no P–O–P bonding was present. The broad band at 613 $cm^{-1}$ and the new band at 744 $cm^{-1}$ can be assigned to B–O–P vibrations[31,46] and those of the 5-membered borate ring, respectively.[30] The other bands observed at ~920 $cm^{-1}$ and 1889 $cm^{-1}$ were assigned to $\nu_a(PO_3)$ ($Q^1$) and C=O stretching of ascorbic acid.[47]

The $^{31}P$ MAS NMR spectra shown in Figure 6 displayed a $Q^1_B$ signal at ca. 25 ppm and broad side bands for **2**, typical for a monophosphate ester. For **3**, $Q^1$ and $Q^2$ resonances of the tripolyphosphate chain appeared as a single, unresolved, strong peak with a shoulder on the high frequency side that can be assigned to $Q^2_B$.

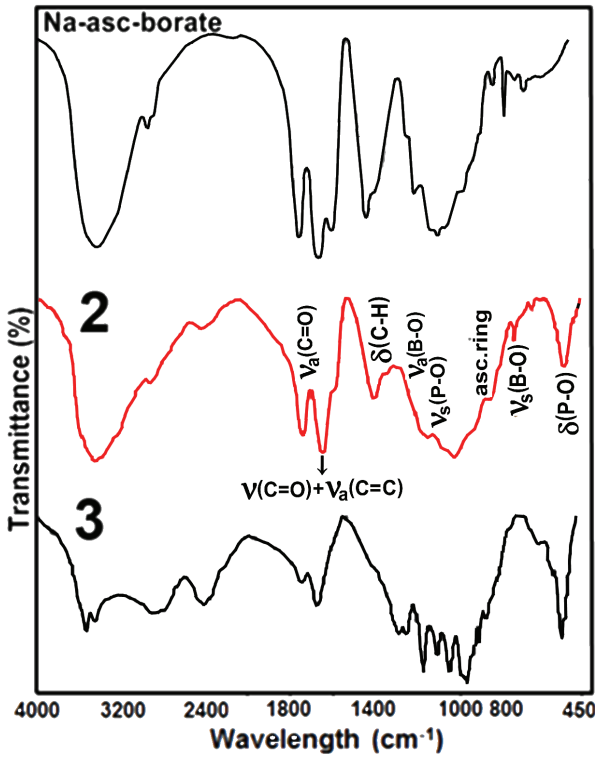


**Figure 5.** FTIR spectra of sodium ascorbatoborate, **2**, and **3**.

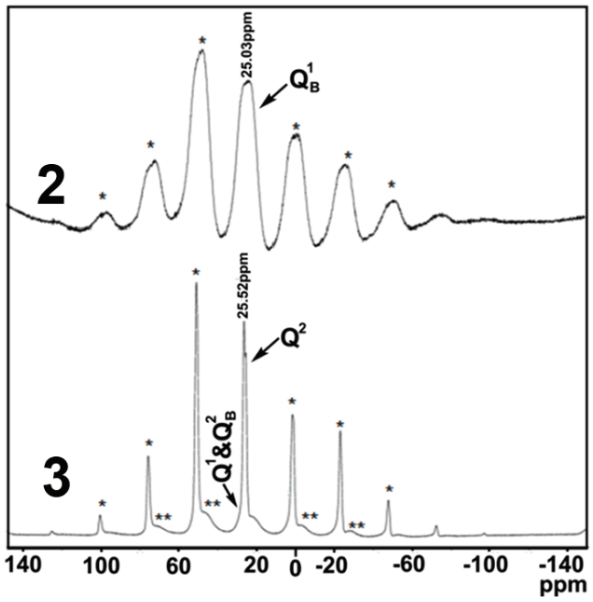


**Figure 6.** $^{31}P$ MAS NMR spectra of **2** and **3**.

Figure 7 shows the $^{11}B$ NMR spectra of **2** and **3** in $D_2O$. The spectra revealed that 3 types of boron species were present in the solutions. The strong peak at $\delta \approx 19$ is due to boric acid resulting from the hydrolysis of the compounds. The weaker signal at ~6 ppm is characteristic for $B_4$ of 5-membered *mono*-chelate rings[41,42] and is normally expected for the undissociated compound. The third signal at ~10 ppm, however, refers to $B_4$ of 5-membered *bis*-chelate rings.[41,48–53] A plausible explanation for the existence of this peak would be the formation of a *bis*-chelate structure between borate and the side chain OH groups of ascorbate while the phosphate group undergoes hydrolytic cleavage. $B_3$:$B_4$ peak area ratio slightly increased on going from **2** to **3** due to the increasing tendency for hydrolysis with a longer phosphate chain.

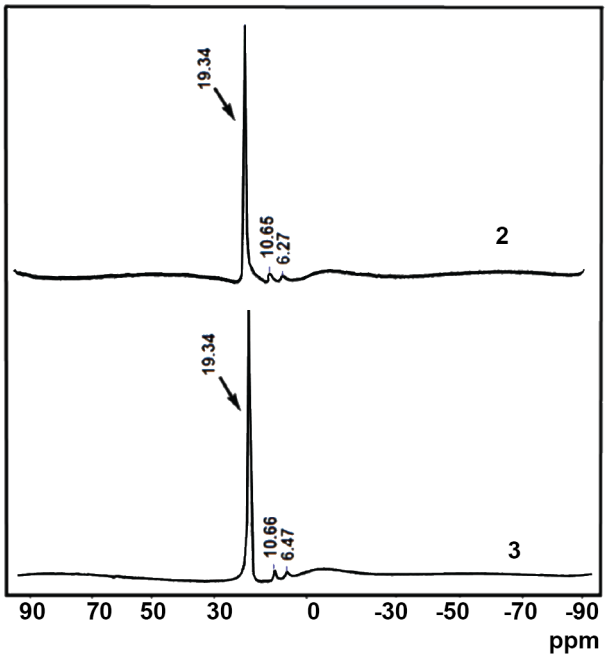


**Figure 7.** $^{11}$B NMR spectra of **2** and **3** in $D_2O$.

Phosphate binding to borate did not cause any effect on the $^{13}$C MAS NMR signals of **2** and **3**. The spectral pattern and the chemical shift values were nearly the same as previously reported for sodium ascorbatoborate.[11] DP mass spectra showed a series of principal ions consistent with the formulae proposed in Figure 1.

**2** and **3** displayed thermal decomposition behaviour similar to that recorded for **1** and both melted with decomposition over a large temperature range. **2** was found to be more stable with a higher decomposition onset temperature (ca. 250 °C) than that of **3** (ca. 200 °C).

### 2.3. Phosphateborate ester of citric acid

Citric acid is an $\alpha$-hydroxycarboxylic acid and forms a 5-membered ring with boron using its central carboxylate and $\alpha$-hydroxy oxygens.[54] Figure 1 represents the proposed structure of the phosphateborate ester of citric acid, based on analytical, spectroscopic, and thermal data. The arguments about the formation of orthophosphate structure for **2** may all apply for **4** on steric grounds.

The FTIR, $^{31}$P MAS NMR, and $^{11}$B NMR spectra of **4** displayed similar characteristics as noted for **2**. The $\nu_a$(C=O) and $\nu_a$(COO) of the citrate group retained their positions at 1733 cm$^{-1}$ and 1581 cm$^{-1}$ as reported for sodium citratoborate.[55,56] Modifications were observed in the region 1200–1000 cm$^{-1}$ due to the incorporation of phosphate into the structure. In this region, individual assignment of the overlapping $\nu_a$(B–O), $\nu_a$(P–O), and $\nu_s$(P–O) bands was difficult; however, the new peak appearing at 958 cm$^{-1}$ would be assigned to B–O–P vibrations. The $Q^2$ band was absent in the Raman spectrum (Figure 2), indicating that that no P–O–P bonding is present. The band at ca. 650 cm$^{-1}$ and the new band at 743 cm$^{-1}$ may be respectively assigned to B–O–P vibrations[31,46] and those of the 5-membered borate ring.[30] The other peaks observed referred to characteristic Raman signals of citric acid.[47] The $^{31}$P MAS NMR and $^{11}$B NMR spectra displayed similar patterns as recorded for **2** with small changes in the chemical shift values due to the structural differences between ascorbic and citric acids. The DP mass spectrum of **4** was consistent with its formulation.

## 3. Conclusions

Possible formation of –C–O–B–O–P– linkages in aqueous media was examined by adding orthophosphate to solutions of boric acid and carboxylic acid functionalised biomolecules. Species containing ortho- to triphosphate groups attached to the borate esters of salicylic, ascorbic, and citric acids were obtained and structurally defined by FTIR, Raman, and NMR studies.

The length of the phosphate chain increased nonlinearly with the amount of $NaH_2PO_4$ employed in the condensation reactions, due to the water-buffered concentration of phosphate species (ortho-, pyro-, or tripolyphosphate) present in the reaction medium.[57] Steric properties of the biomolecule and the nature of the borate chelate could have also played a prominent role in influencing the size of the attached phosphate groups. Orthophosphate structures were obtained with ascorbic and citric acids, which both form 5-membered borate rings and involve side chains that impose steric effects on the attached phosphate group. Salicylic acid, on the other hand, gave a triphosphate product with equimolar reactants, experiencing a less steric repulsion with the planar organic molecule through a 6-membered borate chelate.

The compounds were thermally stable but underwent hydrolytic cleavage in water via disruption of the B–O–P linkages first, followed by the slower hydrolysis of C–O–B linkages as verified by $^{11}$B NMR studies.

While no details of the mechanism are yet available to us, the model studies presented here with carboxylic acids indicate that formation of –C–O–B–O–P– linkages in water can occur under simple conditions. The results suggest a possible role for boron in linking biomolecules to inorganic phosphate providing that the appropriate concentration and pH requirements are established.

## 4. Experimental studies

### 4.1. General

The reagents salicylic acid ($C_7H_6O_3$, Merck), sodium ascorbate ($NaC_6H_7O_6$, Merck), citric acid ($C_6H_8O_7$, Sigma), $NaHCO_3$ (Merck), $H_3BO_3$ (Merck), $NaH_2PO_4.2H_2O$ (Merck), and acetone (Riedel-Haen) were used as received. All experiments were performed in deionised water. Inert reaction conditions and deoxygenated water were employed in experiments with ascorbic acid. C and H contents were determined by a CHNS-932 LECO model analytical instrument. Boron contents were determined by carminic acid method;[58] phosphate analyses were carried out by a DIONEX-ICS-100 model ion chromatograph and sodium analyses by a Jenway PFP:7 flame photometer. Crystal water determination and thermal analyses (thermogravimetric analysis (TGA) and differential thermal analysis (DTA)) were performed by the Shimadzu DTG-60H system, in a dynamic nitrogen atmosphere (15 mL/min), at a heating rate of 10 °C/min, in platinum sample vessels with reference to $\alpha$-$Al_2O_3$. Melting points were determined by an OptiMelt Automated Melting Point System. FTIR spectra were measured in the 450–4000 $cm^{-1}$ range with a PerkinElmer Spectrum One instrument, by using the KBr pellet technique. Raman spectra of samples were recorded using a Labram 800 HR Raman spectrometer (Jobin Yvon) with a He–Ne Laser source emitting at 633 nm, 600–1200 grooves/mm holographic grating, and a charge coupled device (CCD) detector. Solid state $^{13}$C NMR spectra were recorded in 280–0 ppm with a Bruker Avance Ultrashield TM 300 MHz WB instrument, by using a 4-mm MAS probe at 5 kHz spin rate and contact time of 2 ms at 293 K. $^{11}$B NMR spectra were recorded with a Bruker Ultrashield TM 500 MHz instrument in $D_2O$ with reference to $BF_3.Et_2O$. $^{31}$P MAS NMR spectra were recorded with a Bruker UltraShield 300 MHz instrument with reference to $H_3PO_4$ by using a 4-mm MAS probe. The spectrometer frequency was 121.49 MHz and thus 1 ppm amounts to 121.49 Hz. Mass spectra were recorded by an Agilent 5973 Mass Spectrometer in positive ion mode with a direct insertion probe from 40 °C to 450 °C at 5 °C/min.

### 4.2. Reaction conditions

Borate monoesters were prepared in situ by adding solid $H_3BO_3$ to the solutions containing the metal salt of the respective acid in a 1:1 molar ratio, as described previously.[11,19,20,54] After complete dissolution of $H_3BO_3$ was achieved, $NaH_2PO_4.2H_2O$ was added to the solution containing the mono-ester of the bio-acid. The mixture was gently heated and stirred in a rotary evaporator until complete dissolution. The solution was then concentrated to a syrup into which cold acetone was added. The solidified white product was separated, washed with acetone, and dried in a vacuum desiccator. Employing sodium salicylate (8.0 g, 0.05 mol), boric acid (3.1 g, 0.05 mol), and $NaH_2PO_4 \cdot 2H_2O$ (7.8 g, 0.05 mol) (**1**) in 250 mL of water was helpful for product solidification and separation with quantitative yields. The experiments with ascorbic acid were continued with the same conditions employed for **1** (**2**) and by employing a higher amount of $NaH_2PO_4 \cdot 2H_2O$ (23.5 g, 0.15 mol) (**3**), with citric acid (**4**) as for **1**, after converting the acids into their corresponding mono sodium salts. All the products were obtained as white hygroscopic powders with high solubility in water.

### 4.3. Characterisation data

Schematic structures for **1**–**4** are shown in Figure 1; experimental data for them are given below.

**1.** Found (%): C 12.89, H 2.36, B 1.82, P 16.20, Na 16.8, $H_2O$ ca. 16.0. Calculated for $BC_7H_6Na_4P_3O_{14}.6H_2O$ (MW 618 g mol$^{-1}$) (%): C 13.59, H 2.91, B 1.78, P 15.05, Na 14.89, $H_2O$ 17.47. mp 330 °C. $^{11}$B/ppm: 19.2, 2.8. $^{31}$P/ppm: 22.45. IR/cm$^{-1}$: 1692, 1614, 1482, 1351, 1263, 1250, 1150, 1075, 976, 753, 695, 530. Raman/cm$^{-1}$: 590, 641, 995, 1167. MS/$m/z$: 486, 303, 264, 236, 164.

**2.** Found (%): C 18.09, H 3.25, B 3.21, $H_2O$ ca. 10.0. Calculated for $BC_6H_{10}Na_2PO_{11}.2H_2O$ (MW 380 g mol$^{-1}$) (%): C 18.94, H 3.68, B 2.89, $H_2O$ 9.47. mp 140 °C. $^{11}$B/ppm: 19.3, 10.6, 6.3. $^{31}$P/ppm: 25.03. $^{13}$C/ppm: 169, 147, 110, 70, 62, 57. IR/cm$^{-1}$: 1748, 1655, 1408, 1300–850 (broad), 760, 518. Raman/cm$^{-1}$: 613, 744, 914, 929. MS/ m/$z$ 279, 256, 236, 185, 167, 97, 83, 44.

**3.** Found (%): C 11.18, H 2.87, B 2.20, $H_2O$ ca. 11.0. Calculated for $BC_6H_{10}Na_4P_3O_{17}.4H_2O$ (MW 621 g mol$^{-1}$) (%): C 11.59, H 2.90, B 1.77, $H_2O$ 11.59 mp 128 °C. $^{11}$B/ppm: 19.3, 10.6, 6.5. $^{31}$P/ppm: 26.52. IR/cm$^{-1}$: 1750, 1655, 1400–800 (broad), 525.

**4.** Found (%): C 17.89, H 2.89, B 2.40, $H_2O$ ca. 10.0. Calculated for $BC_6H_{10}Na_2PO_{11}.2H_2O$ (MW 396 g mol$^{-1}$) (%): C 18.18, H 3.53, B 1.77, $H_2O$ 9.09. mp 122 °C.

$^{11}$B/ppm: 19.4, 9.1, 5.2. $^{31}$P/ppm: 25.56. IR/cm$^{-1}$: 1733, 1406, 1323, 1119, 958, 517. Raman/cm$^{-1}$: 214, 380, 557, 564, 743, 915, 928, 1029, 1078, 1102, 1129, 1158. MS/$m/z$ 337, 321, 97, 44.

### Acknowledgements

This work was financially supported by the Scientific and Technological Research Council of Turkey (project: 109T904). The authors acknowledge Prof Ali Güner and Dr Serap Kavlak for recording the Raman spectra, and Prof Bekir Salih and Dr Ömür Çelikbiçak for the DP-MS spectra.

### References

1. Cairns-Smith, A. G. *Seven Clues to the Origin of Life*, Cambridge University Press: Cambridge, UK, 1985.
2. Fitz, D.; Reiner, H.; Rode, B. M. *Pure Appl. Chem.* **2007**, *79*, 2101–2117.
3. Arrhenius, G.; Sales, B.; Mojzsis, S.; Lee, T. *J. Theor. Biol.* **1987**, *187*, 503–522.

4. Arrhenius, G. O. *Helv. Chim. Acta* **2003**, *86*, 1569–1586.
5. Schwartz, A. W. *Phil. Trans. R. Soc. B.* **2006**, *361*, 1743–1749.
6. Ricardo, A.; Carrigan, M. A.; Olcott, A. N.; Benner, S. A. *Science* **2004**, *303*, 196.
7. Amaral, A. F.; Marques, M. M.; da Silva, J. A. L.; da Silva, J. J. R. F. *New J. Chem.* **2008**, *32*, 2043–2049.
8. Scorei, R. *Orig. Life Evol. Biosph.* **2012**, *42*, 3–17.
9. Prieur, B. E. *C. R. Acad. Sci. Ser. IIC Chem.* **2001**, *4*, 667–670.
10. Scorei, R.; Cimpoiasu, V. M. *Orig. Life Evol. Biosph.* **2006**, *36*, 1–11.
11. Köse, D. A.; Zümreoglu-Karan, B. *New J. Chem.* **2009**, *33*, 1874–1881.
12. Saladino, R.; Barontini, M.; Cossetti, C.; Di Mauro, E.; Crestini, C. *Orig. Life Evol. Biosph.* **2011**, *41*, 317–330.
13. Holm, N. G.; Dumont, M.; Ivarsson, M.; Konn, C. *Geochem. T.* **2006**, *7*, 1–7.
14. Nikonov, G. N.; Balyeva, A. S. *Russ. Chem. Rev.* **1992**, *61*, 335–351.
15. Hauf, C.; Kniep, E. R. *Z. Kristallogr.* **1996**, *211*, 705–706.
16. Boy, I.; Hauf, C.; Kniep, R. *Z. Naturforsch B* **1998**, *53*, 631–633.
17. Bontchev, R. P.; Sevov, S. C. *Inorg. Chem.* **1996**, *35*, 6910–6911.
18. Li, M. R.; Mao, S. Y.; Huang, Y. X.; Mi, J. X.; Wei, Z. B.; Zhao, J. T.; Kniep R. *Z. Krist. - New Cryst. St.* **2002**, *217*, 165–166.
19. Köse, D. A.; Zümreoglu-Karan, B.; Hökelek, T.; Sahin, E. *Inorg. Chim Acta* **2010**, *363*, 4031–4037.
20. Köse, D. A.; Zümreoglu-Karan, B.; Hökelek, T. *Inorg. Chim. Acta* **2011**, *375*, 236–241.
21. Chvertkina, L. V.; Khoklov, P. S.; Mironov, V. F. *Russ. Chem. Rev.* **1992**, *61*, 1009–1021.
22. Van Duin, M.; Peters, J. A.; Kieboom, A. P. G.; Van Bekkum, H. *Tetrahedron* **1984**, *40*, 2901–2911.
23. Kulaev, I. S.; Vagabov, V. M.; Kulakovskaya, T. V. *The Biochemistry of Inorganic Polyphosphates*, Wiley: New York, NY, USA, 2004, pp. 3–14.
24. Kirkpatrick, R. J.; Brow, R. K. *Solid State Nucl. Mag. Res.* **1995**, *5*, 9–21.
25. Wiench, J. M.; Pruski, M.; Tischendorf, B.; Otaigbe, J. U.; Sales, B. C. *J. Non-Cryst. Solids* **2000**, *263*, 101–110.
26. Carta, D.; Qiu, D.; Guerry, I.; Ahmed, P.; Abou Neel, E. A.; Knowles, J. C.; Smith, M. E.; Newport, R. J. *J. Non-Cryst Solids* **2008**, *354*, 3671–3677.
27. Peak, D.; Luther, G. W.; Sparks, D. L. *Geochim. Cosmochim. Acta* **2003**, *67*, 2551–2560.
28. Efimov, A. M. *J. Non-Cryst. Solids* **1997**, *209*, 209–226.
29. Saranti, A.; Koutselas, I.; Karakassides, M. A. *J. Non-Cryst. Solids* **2006**, *352*, 390–398.
30. Oertel, R. P. *Inorg. Chem.* **1972**, *11*, 544–549.
31. Gaylord, S.; Tincher, B.; Petit, L.; Richardson, K. *Mater. Res. Bull.* **2009**, *44*, 1031–1035.
32. Kim, N. J.; Im, S. H.; Kim, D. H.; Yoon, D. K.; Ryu, B. K. *Electron. Mater. Lett.* **2010**, *6*, 103–106.
33. Turner, B. L.; Mahieu, N.; Condron, L. M. *Soil Sci. Soc. Am. J.* **2003**, *67*, 497–510.
34. Brow, R. K. *J. Non-Cryst. Solids* **2000**, *263 & 264*, 1–28.
35. Munoz, F.; Montagne, L.; Pascual, L.; Duran, A. *J. Non-Cryst. Solids* **2009**, *355*, 2571–2577.
36. Shah, K. V.; Goswami, M.; Deot, M. N.; Sarkar, A.; Manikandan, S.; Shrikhande, V. K.; Kothiyal, G. P. *Bull. Mater. Sci.* **2006**, *29*, 43–48.
37. Grimmer, A. R.; Müller, D.; Gözel, G.; Kniep, R. *Fresen. J. Anal. Chem.* **1997**, *357*, 485–488.
38. Elbers, S.; Strojek, W.; Koudelka, L.; Eckert, H. *Solid State Nucl. Magn. Reson.* **2005**, *27*, 65–76.
39. Beckett, M. A.; Rugen-Hankey, M. P.; Varma, K. S. *J. Sol-Gel Sci. Techn.* **2006**, *39*, 95–101.

40. Kennedy, J. D. In: Mason J. (ed) *Multinuclear NMR*, Plenum: New York, NY, USA, 1987, 221-253.
41. Bishop, M.; Shahid, N.; Yang, J.; Barron, A. R. *Dalton Trans.* **2004**, *7*, 2621–2634.
42. Tossell, J. A. *Geochim. Cosmochim. Acta* **2006**, *70*, 5089–5103.
43. Köse, D. A.; Zümreoglu-Karan, B. *Chem. Pap.* **2012**, *66*, 54–60.
44. Michelmore, A.; Gong, W.; Jenkins, P.; Ralston, J. *Phys. Chem. Chem. Phys.* **2000**, *2*, 2985–2992.
45. Gong, W. *Int. J. Miner. Process.* **2001**, *63*, 147–165.
46. Vyatchina, V. G.; Perelyaeva, L. A.; Zuev, M. G.; Mamoshin, V. L. *Glass. Phys. Chem.* **2003**, *29*, 522–525.
47. De Gelder, J.; De Gussem, K.; Vandenabeele, P.; Moens, L.; *J. Raman Spectrosc.* **2007**, *38*, 1133–1147.
48. Matsunaga, T.; Nagata, T. *Anal. Sci.* **1995**, *11*, 889–892.
49. Shao, C. Y.; Matsuoka, S.; Miyazaki, Y.; Yoshimura, K. *Anal. Sci.* **2001**, *17*, i1475–i1478.
50. Beckett, M. A.; Bland, C. C.; Varma, K. S. *Polyhedron* **2008**, *27*, 2226–2230.
51. Dawber, J. G.; Green, S. I. E. *J. Chem. Soc. Faraday Trans.I* **1986**, *82*, 3407–3413.
52. Dawber, J. G. *J. Chem. Soc. Faraday Trans. I* **1987**, *83*, 771–777.
53. Dawber, J. G.; Green, S. I. E.; Dawber, J. C.; Gabrail, S. *J. Chem. Soc. Faraday Trans. I* **1988**, *84*, 41–45.
54. Köse, D. A. Dissertation, Hacettepe University, Turkey, 2008.
55. Zviedre, I. I.; Belyakov, S. V. *J. Struct. Chem.* **2009**, *50*, 114–119.
56. Zviedre, I. I.; Belyakov, S. V. *Russ. J. Inorg. Chem.* **2009**, *54*, 1390–1395.
57. Pasek, M. A. *P. Natl. Acad. Sci. USA* **2008**, *105*, 853–858.
58. Weicher, F. H. *Standard Methods of Chemical Analysis, Part B, 6th edn.* Van Nostrand: New York, NY, USA, 1963, pp. 2406–2407.